

Galaxy Zoo: the fraction of merging galaxies in the SDSS and their morphologies

D. W. Darg,^{1*} S. Kaviraj,^{2,1†} C. J. Lintott,^{1‡} K. Schawinski,^{3,4} M. Sarzi,⁵ S. Bamford,⁶ J. Silk,¹ R. Proctor,⁷ D. Andreescu,⁸ P. Murray,⁹ R. C. Nichol,¹⁰ M. J. Raddick,¹¹ A. Slosar,¹² A. S. Szalay,¹¹ D. Thomas,¹⁰ J. Vandenberg.¹¹ §

¹ Department of Physics, University of Oxford, Keble Road, Oxford, OX1 3RH, UK

² Mullard Space Science Laboratory, University College London, Holmbury St. Mary, Dorking, Surrey RH5 6NT, UK

³ Department of Physics, Yale University, New Haven, CT 06511, USA

⁴ Yale Center for Astronomy and Astrophysics, Yale University, P.O. Box 208121, New Haven, CT 06520, USA

⁵ Centre for Astrophysics Research, University of Hertfordshire, Hatfield, AL10 9AB, UK

⁶ Centre for Astronomy and Particle Theory, University of Nottingham, University Park, Nottingham, NG7 2RD, UK

⁷ Waveney Consulting/Waveney Web Services, 28 Diprose Road, Corfe Mullen, Wimborne, Dorset, BH21 3QY, UK

⁸ LinkLab, 4506 Graystone Ave., Bronx, NY 10471, USA

⁹ Fingerprint Digital Media, 9 Victoria Close, Newtownards, Co. Down, Northern Ireland, BT23 7GY, UK

¹⁰ Institute of Cosmology and Gravitation, University of Portsmouth, Mercantile House, Hampshire Terrace, Portsmouth, PO1 2EG, UK

¹¹ Department of Physics and Astronomy, Johns Hopkins University, 3400 N. Charles St., Baltimore, MD 21218, USA

¹² Berkeley Center for Cosmological Physics, Lawrence Berkeley National Laboratory and Physics Department, University of California, Berkeley CA 94720, USA

15 November 2019

ABSTRACT

We present the largest, most homogeneous catalogue of merging galaxies in the nearby universe obtained through the Galaxy Zoo project - an interface on the world-wide web enabling large-scale morphological classification of galaxies through visual inspection of images from the Sloan Digital Sky Survey (SDSS). The method converts a set of visually-inspected classifications for each galaxy into a single parameter (the ‘weighted-merger-vote fraction’, f_m) which describes our confidence that the system is part of an ongoing merger. We describe how f_m is used to create a catalogue of 3003 visually-selected pairs of merging galaxies from the SDSS in the redshift range $0.005 < z < 0.1$. We use our merger sample and values of f_m applied to the SDSS Main Galaxy Spectral sample (MGS) to estimate that the fraction of volume-limited ($M_r < 20.55$) major mergers ($1/3 < M_1^*/M_2^* < 3$) in the nearby universe is 1 – 3%. Having visually classified the morphologies of the constituent galaxies in our mergers, we find that the spiral-to-elliptical ratio of galaxies in mergers is higher by a factor ~ 2 relative to the global population. In a companion paper, we examine the internal properties of these merging galaxies and conclude that this high spiral-to-elliptical ratio in mergers is due to a longer time-scale over which mergers with spirals are detectable compared to mergers with ellipticals.

Key words: catalogues – Galaxy:interactions – galaxies:evolution – galaxies: general – galaxies:elliptical and lenticular, cD – galaxies:spiral

* Email: ddarg@astro.ox.ac.uk

† Email: skaviraj@astro.ox.ac.uk

‡ Email: cjl@astro.ox.ac.uk

§ This publication has been made possible by the participation of more than 140,000 volunteers in the Galaxy Zoo

project. Their contributions are individually acknowledged at <http://www.galaxyzoo.org/Volunteers.aspx>.

1 INTRODUCTION

1.1 Mergers in Contemporary Research

Galaxy mergers and interactions are connected to many pressing questions concerning the origin, evolution and properties of cosmic structures. These issues include the formation of galaxies (White & Rees 1978; Lacey & Cole 1993; Conselice 2006a; De Lucia et al. 2006), environmental effects on morphology (Capak et al. 2007; Park et al. 2007; Ball et al. 2008; Van der Wel 2008) and the distribution of the dark matter that drives the merger process (Bond et al. 1991; Cole et al. 2000; Fakhouri & Ma 2008). At the sub-galactic scale mergers have been invoked to explain a variety of observations, notably localised bursts of star formation (Kennicutt et al. 1987; Schweizer et al. 2005; Di Matteo et al. 2005; Woods & Geller 2007; Barton et al. 2007; Li et al. 2008; Cox et al. 2008) and induced nuclear activity (Keel et al. 1985; Schawinski et al. 2007a; Jogee 2008). The far-reaching effects that mergers are thought to produce makes their empirical examination an important task.

To date though, such studies have concentrated mostly on merger *rates* (Carlberg et al. 2000; Le Fevre et al. 2000; Patton et al. 2002; Conselice et al. 2003; Bundy et al. 2005; Bell et al. 2006; Conselice, Rajgor & Myers 2008; Lin et al. 2008; Lotz et al. 2008a; Hsieh et al. 2008, Patton et al. 2008), with comparatively little carried out to examine their morphologies and internal properties (though see Li et al. 2008; Ellison et al. 2008) for reasons to be discussed (§1.2). This is unfortunate. To understand the exact role played by mergers in galaxy evolution, it is inadequate to measure their rates alone since the processes that determine the morphological outcomes of mergers are still not fully understood.

It has been widely believed since the simulations of Toomre & Toomre (1972) that two spirals *can* merge to form an elliptical but this does not mean that they *must*. On the contrary, recent studies have argued convincingly that, in some cases at least, disc galaxies are able to survive (multiple) major mergers (Hopkins et al. 2009). Where this does happen, the probability of disc survival must be assumed *a priori* to depend on the properties of its progenitors such as environment, gas content and feedback mechanisms. These in turn correlate with galactic morphology. There is also good reason to think that the time-scales over which mergers are detectable depends on the internal properties of the progenitors (Lotz et al. 2008b). Ideally then, calculations that convert merger fractions into merger rates as part of some hierarchical-structure scheme (such as modelled by Khochfar & Burkert 2003) should take the properties and morphologies of their sample into account. Only then can models of hierarchical galaxy formation be fully tested.

The Galaxy Zoo project contributes to this important task by providing a snapshot of mergers as they appear in the local universe ($0.005 < z < 0.1$). Plans are also underway to apply the same merger-locating system to higher redshift surveys. In this paper we present a simple but powerful method for identifying mergers using the world-wide web and a robust sample of 3003 merging systems obtained

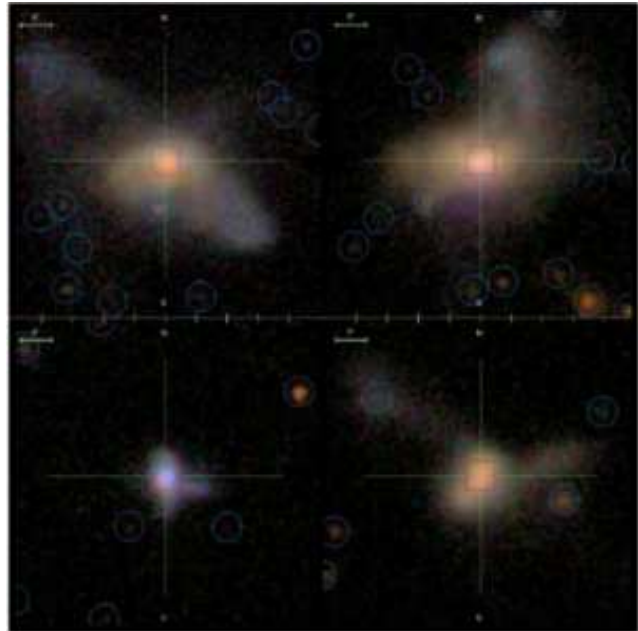


Figure 1. Example images of ‘strongly-perturbed’ systems which are not deblended into two photometric objects that plausibly represent the photometry of the progenitors. These are usually late-stage mergers and cannot be detected by the close-pairs technique.

by it (§2.1).¹ We then discuss three important ratios revealed by this study: the merger fraction of the local universe (§3), the fraction of spectral pairs in merging systems in SDSS (relevant to discussions for the close-pairs technique; §3.4) and the spiral-to-elliptical ratio of galaxies that are in merging systems (§3.5). In the companion paper, Darg et al. 2009 (D09b from here on), we present the environment and internal properties of these merging galaxies.

Galaxy Zoo is a new player in the game of merger-location techniques. Before describing our results, we begin with a description of current methods used to find mergers so that the role and value of Galaxy Zoo can be understood in the context of contemporary research.

1.2 Locating Mergers: Past Methods

Visual inspection remains the most trustworthy way of determining whether or not a galaxy is merging. However, the advent of large galaxy surveys such as SDSS (York et al. 2000) involving $\sim 10^6$ objects has rendered classification by individual researchers impractical. Automated methods have therefore been developed to approximate the human decision making process but, being only approximations, encounter certain difficulties that Galaxy Zoo can help overcome.

¹ We have labelled this catalogue GZM1 (Galaxy-Zoo Mergers 1).

1.2.1 Close-Pair Statistics

Accurate measures of position and redshift in large scale surveys have made straightforward the task of finding close pairs in the (local) universe. However, the peculiar velocities of the individual galaxies can significantly offset their redshift-inferred line-of-sight separation producing spectral pairs of non-interacting systems which may or may not merge. One can apply statistical arguments as to what fraction of close-pairs within some ensemble will soon merge, but no single system can be safely assumed to be merging without cross-examination. The method is best used, therefore, to estimate merger *rates* parametrised by the convention $rate \sim (1+z)^m$.

Another limitation of close-pairs methods in surveys such as SDSS is the requirement that *both* galaxies have spectra. This requires a delicate act of deblending by the data-reduction pipeline. SDSS will convert the photometry of an extended body like a galaxy (the ‘parent’) into individual photometric ‘objects’ (the ‘children’) depending on how many peaks are present in the blended image (Stoughton et al. 2002). Iterations are performed allotting different magnitudes to the child-objects until an optimal distribution is attained so that all children sum to give the total flux of the parent.

Only if a contiguous body, such as two interacting galaxies, is deblended into (at least) two photometric objects both having Petrosian magnitudes $r < 17.77$ can it contain two spectral targets. Mergers with only one deblended object of $r < 17.77$ can not be identified by the close-pairs technique (Strauss et al. 2002; Patton et al. 2008). This will occur for many minor mergers or for late stage mergers where the cores have drawn close to each other and the pipeline reads them as a single peak. Figure 1 shows examples of strongly-perturbed systems with only one spectral target.

Even when two objects are deblended in a contiguous image and registered as spectral targets - relatively few systems will obtain spectra on *both* objects due to fiber collisions within the spectrometer. Two SDSS spectroscopic targets cannot acquire spectra simultaneously if they are within $55''$ of each other and so only systems contained within ‘tile overlap regions’ can have spectral objects with an angular separation less than this (Strauss et al. 2002, Blanton et al. 2003). Only about $\sim 30\%$ of the SDSS sky rests within overlap regions thus limiting the sample size of such systems.

Conversely, a system deblended into multiple targets, as in Figure 2, can acquire too many spectral objects so that a single galaxy might appear as a close-pair or a binary merger might appear as a multi-merger. Close-pairs studies typically limit the redshift and magnitude ranges in order to avoid this effect. Woods & Geller (2007), for example, limit their close-pairs sample to $\sim 0.027 < z < 0.17$ and require $> 20\%$ of the galaxy’s total flux land within the fiber aperture in order to exclude very extended nearby galaxies. They still find though that $\sim 15\%$ of their minor-pairs catalogue are false pairs after visual inspection.

To summarise, without visual cross-examination, close-pairs methods are prone to include false pairs and non-gravitationally bound systems and are best used, therefore, to estimate merger *rates* via application to large ensembles after estimations for contamination and incompleteness are taken into account. To examine the *properties* of merger sys-

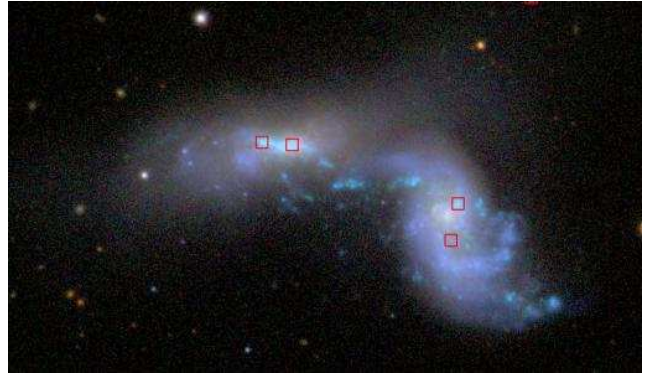


Figure 2. Example image of binary merger with four spectral objects. It is difficult for ‘blind’ close-pairs techniques to distinguish this from a pair of binary pairs (or a four-way merger).

tems, one should robustly identify *actual* mergers as opposed to claims that some fraction of an ensemble is ‘likely’ to be merging.

1.2.2 Automated Quantification of Morphological Disturbance

Pattern recognition techniques applied to galaxy images pose a formidable programming challenge. Background noise and contaminants first need to be removed, then an automated technique needs to quantify how ‘disturbed’ a morphology is independent of viewing angle. This might not be so difficult if it were not the case that unperturbed galaxies themselves vary so much from the structurally simple (ellipticals) to the complex (spirals). In particular, filtering asymmetric systems like mergers from spirals with extended star-formation requires great finesse.

Nonetheless, promising automated techniques have been developed in recent years that generate parameters related to morphology. A common technique has been to measure concentration (C), asymmetry (A) and, in some cases, clumpiness/smoothness (S). One then partitions CA(S) space into morphological categories and identifies an object as a merger if it lies within the designated sub-volume (see Conselice 2003 and Conselice et al. 2003 on the use of the ‘CAS’ system to locate mergers).

Another pair of parameters used in this fashion are the Gini-coefficient (G) (Abraham et al. 2003) and second-order moment of the brightest 20% of the galaxy’s light (M_{20}), most notably by Lotz et al. (2008a). (For a concise description of how to calculate C, A, S, G and M_{20} see Conselice, Rajgor & Myers 2008.) It is argued in Lotz, Primack & Madau (2004) that this technique operates better at low signal-to-noise ratios and is more sensitive to late-stage morphologies than the CAS system (though see Lisker 2008 for a critique of its effectiveness). More recent studies have combined and compared the two techniques (e.g. Scarlata et al. 2007; Conselice, Rajgor & Myers 2008; Lotz et al. 2008b). Artificial Neural Nets are another promising technique for identifying morphologies (Lahav et al. 1996, Ball et al. 2004) though they have not yet been applied to merger studies specifically.

CAS and GM_{20} remain effective at high redshifts so long as the image quality remains high and, since they are

automated, can process images quickly once the pipeline has been established. However, these techniques also require visual examination to cross-check results and to fine-tune the partition boundaries that define a merger.

Systematic uncertainties usually remain. Jogee et al. (2008) recently report that the CAS criterion failed to pick up 37 – 58% of their visually classified “strongly disturbed” morphologies while including a “significant number of relatively normal galaxies” - an effect that was predicted by simulations in Conselice (2006b). Conselice, Rajgor & Myers (2008) recently classified 993 images from the Hubble-Ultra-Deep Field by visual inspection, the CAS volume and the GM₂₀ area. They found some notable disagreements, in particular, some systems identified as mergers by their location in GM₂₀ space are not identified as mergers using the CAS system and vice-versa (see for example Figures 8 and 9 plus captions). Within the $0.4 < z < 0.8$ range only $44 \pm 6\%$ of the galaxies mapped into the GM₂₀ merger region were visually classified as ‘peculiar.’

Recently Lotz et al. (2008b) performed an extensive study on the merger-detection sensitivity of the CA, GM₂₀ and close-pairs techniques using simulations. They find that C, A, G and M₂₀ methods are only sensitive to mergers at specific stages of the process, particularly the first pass and final coalescence of the galaxies. The study also confirms that the merger time-scales and parameters (such as gas-fractions, pericentric distance and relative orientation) for which these three techniques remain sensitive differ significantly.

Evidently then, much work remains before we can confidently do away with visual inspection of images in merger studies.²

1.2.3 Visual Inspection by Research Groups

In the pre-digital age, surveys of morphological classification by visual inspection were mostly limited to studies based on cluster images (Oemler 1974, Dressler 1980). With the modern development of large surveys and high resolution imaging, the potential to extract large samples of morphologically classified galaxies in differing environments has vastly improved. The largest visual classification project by a research group is Schawinski et al. (2007a) who visually examined 48,023 SDSS galaxies in compiling the MOSES catalogue (MORphologically Selected Ellipticals in SDSS). They found a significant blue-population that had been excluded by studies such as Bernardi et al. (2003) which identified ellipticals by their presumed properties. Selecting morphologies by *a priori* assumptions is often pragmatic and necessary but ultimately begs the question as to what the properties of a given morphology actually are. Unless we can be certain that a set of properties maps one-to-one with morphology we must continue with visual examination.

Studies to select *mergers* by visual-selection have not reached such scales as MOSES until this work. Le Fevre et al. (2000) visually examined 285 Hubble images and found a merger fraction of $10 \pm 2\%$ over $0 < z \lesssim 1.2$. Nakamura et al. (2003) visually classified 2418 images of

SDSS galaxy objects with Petrosian $r < 16.0$ (i.e. low redshift) finding that 35/1875 of their morphological classifications were Im (‘highly irregular’ following Hubble’s notation). A similar study by the same group, Fukugita et al. (2007), visually classified 2658 images from SDSS with Petrosian $r < 15.9$ and found that 1.5% – 1.7% of these nearby magnitude limited galaxies were ‘interacting.’

Thus, until now, merger studies have been limited to catalogues of $\sim 10^3$ galaxies due to the time-consuming and monotonous nature of the task. By contrast Galaxy Zoo allows us to acquire effective visual classification for morphologies and mergers for samples of $\sim 10^5$ galaxies with relative ease.

1.3 Locating Mergers with Galaxy Zoo

Galaxy Zoo (GZ) is a user interface on the world-wide web³ drawing upon images from SDSS. Volunteers from the public are instructed and commissioned with the collective task of visual classification of $\sim 900,000$ galaxies from SDSS. A complete description of the project including design details and initial data reduction is given by Lintott et al. (2008). It is also shown that public users are, in large numbers, about as good as ‘experts’ at identifying morphologies.

The project has proved to be a tremendous success. To date, over 140,000 volunteers have participated and collectively offered classifications for all $\sim 900,000$ images, on average, fifty times over. Data from the project has already been employed to find the statistical properties of spiral-galaxy-spin orientation (Land et al. 2008; Slosar et al. 2009), the relationships between environment, morphology and colour (Bamford et al. 2008a; Skibba et al. 2008) and to study optically blue early-type galaxies at very low redshift (Schawinski et al. 2009). This work concentrates on the results of the merger-location functionality of Galaxy Zoo whose details we now describe.

2 THE GALAXY ZOO DATA

2.1 Constructing a Binary Merger Catalogue

Galaxy-Zoo users are asked to classify an SDSS target as

- (i) elliptical (e)
- (ii) spiral (s)⁴
- (iii) star/bad image (b), or
- (iv) merger (m).

The Galaxy Zoo project is the first of its kind and so, not knowing how well it would be taken up by the public, the design of the interface prioritised simplicity over detail. A single button labelled ‘merger’ is all that was offered.

The raw data we use to build our catalogue is what we call the *weighted-merger-vote fraction* (f_m). GZ has obtained a value for this parameter for 893,292 SDSS galaxies from

² “Men trust their ears less than their eyes.” Herodotus, *The Histories*, 5th c. B.C., 1.8, trans D. Godley.

³ <http://www.galaxyzoo.org/>

⁴ More specifically, users are asked to specify whether a spiral galaxy is rotating clockwise, anti-clockwise or is edge-on/unclear.

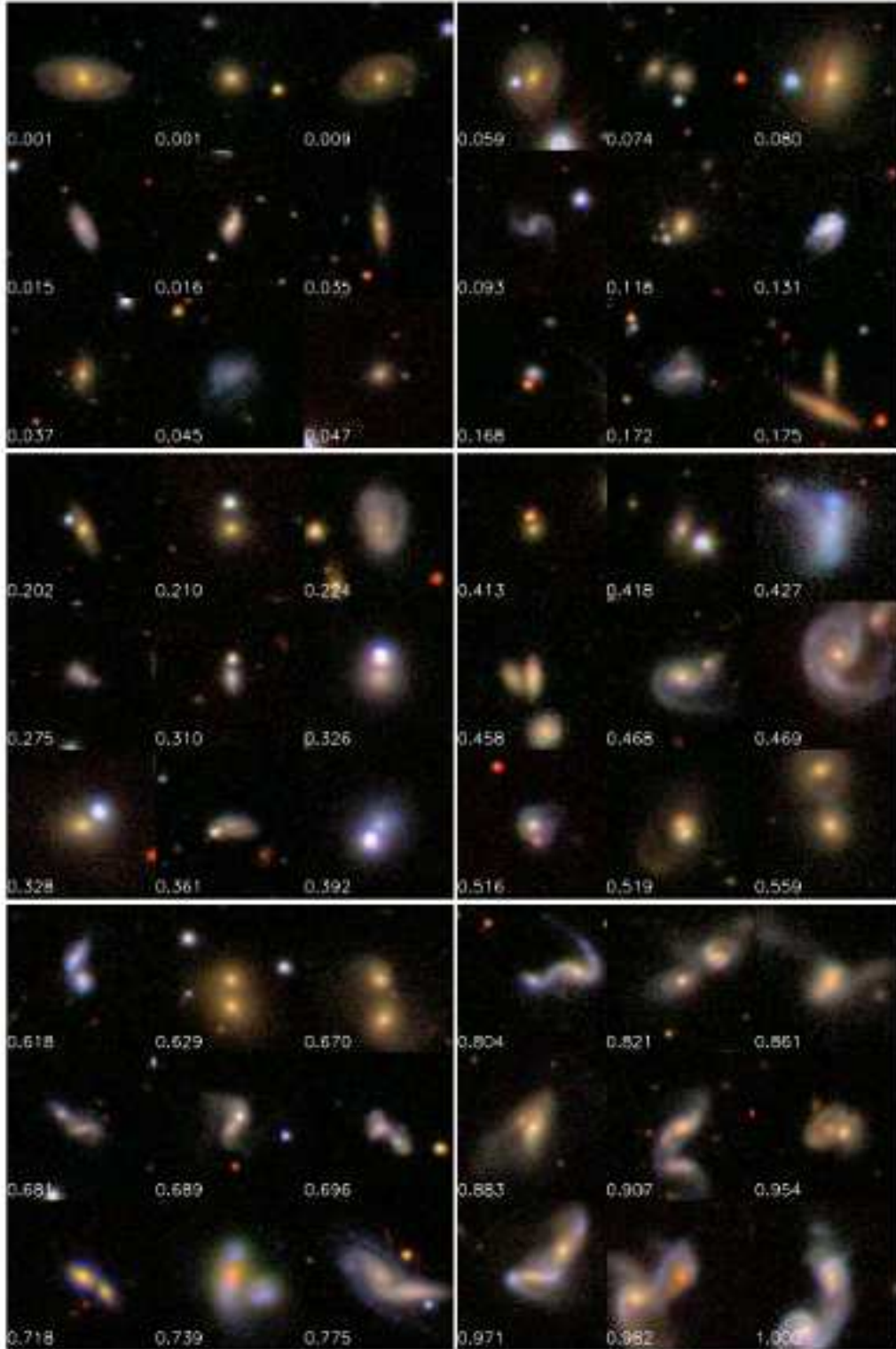


Figure 3. Example images of prospective merger systems. The number given for each image is its weighted-merger-vote fraction, f_m . The panels of nine images are grouped into the following bins: top-left: $0 < f_m \leq 0.05$, top-right: $0.05 < f_m \leq 0.2$; middle-left: $0.2 < f_m \leq 0.4$, middle-right: $0.4 < f_m \leq 0.6$; bottom-left: $0.6 < f_m \leq 0.8$, bottom-right: $0.8 < f_m \leq 1.0$. Our catalogue is made up of mergers with $f_m > 0.4$. Each image tile is $40'' \times 40''$.

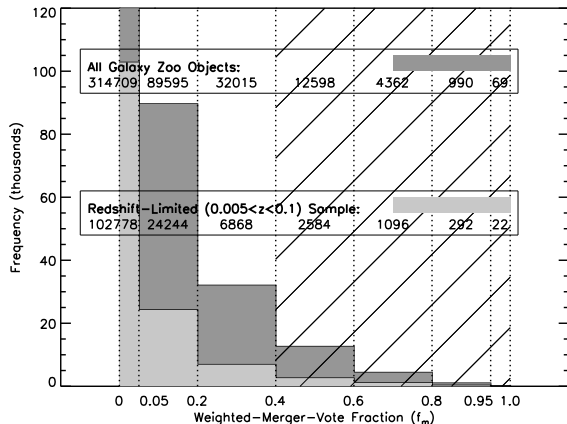


Figure 4. The distribution of weighted-merger-vote fractions in the Galaxy Zoo database. We use spectroscopic objects with $0.005 < z < 0.1$ and $0.4 < f_m \leq 1.0$ to construct our binary-mergers catalogue (cross-hatched). 285,869 Galaxy Zoo spectral objects lie between $0.005 < z < 0.1$, 147,984 of which have $f_m = 0$.

DR6.⁵ The f_m values are calculated by taking the number of *merger* classifications (n_m) for a given GZ object and dividing it by the *total* number of classifications ($n_{e,s,b,m}$) for that object multiplied by a weighting factor W that measures the quality of the particular users that have assessed the object. The quality of an individual user is determined by measuring to what extent that person agrees with the majority opinion for all objects the individual has viewed. The weighting factor, W , thereby represents all the iterations carried out by equations (1) & (2) of Lintott et al. (2008).⁶

$$f_m = \frac{W n_m}{n_{e,s,b,m}}. \quad (1)$$

The parameter f_m ranges from 0 to 1 so that an object with $f_m = 0$ should look nothing like a merger and $f_m = 1$ should look unmistakably so. Figure 3 shows some example images taken from GZ labelled by their f_m values. It is somewhat surprising to see how low f_m is when these images start to look, at least superficially, like mergers ($f_m \sim 0.2 - 0.4$). Evidently, users were rather conservative in calling something a merger.

Figure 4 shows the distribution of f_m for the entire GZ catalogue. In building our first merger catalogue we determined a cut-off point for f_m above which most systems will be proper galactic mergers and involve a sample size manageable by a research team. By comparing the merger-vote fraction with images like those in Figure 3, we decided to build our first catalogue using only systems with $f_m > 0.4$ and only using GZ objects with spectra whose spectroscopic redshift lies in the range $0.005 < z < 0.1$. SDSS spectroscopic targets are selected for galaxies with magnitude

$r < 17.77$ which corresponds to $M_r < -20.55$ at $z = 0.1$. This absolute magnitude corresponds to a minimum stellar mass of $\sim 10^{10} M_\odot$ (see Figure 9) so that our upper limit ($z = 0.1$) is inclusive of intermediate size galaxies. The resolution of images beyond $z > 0.1$ is also rapidly diminishing which would lead to unreliable visual classifications of morphology.

The lower limit $z = 0.005$ is to minimise the number of mergers that go undetected due to an incomplete field of view.⁷ These cases are rare since the number of SDSS objects peaks near $z = 0.08$ and only a few percent have $z < 0.02$.

Within these ranges ($0.005 < z < 0.1$; $0.4 < f_m \leq 1.0$) we have 3994 GZ objects with spectra. We exclude those SDSS targets which are yet to acquire spectra as we desire accurately measured redshifts. Mergers are inherently ‘messy’ systems and so photometric redshifts calculated by comparison to standard templates are prone to error. In fact we found the *mean* absolute difference between all the photometric and spectroscopic redshifts in our merger sample to be ~ 0.051 - more than half of our redshift range.

Although the purpose of the Galaxy Zoo project is to significantly reduce the need for research teams to visually inspect large catalogues, it is still necessary at this stage to double check the results. Visual re-examination of the sample by our group allowed us to

- (i) remove any non-merging systems,
- (ii) visually select an appropriate SDSS object to represent the merging partner, and
- (iii) assign morphologies to the galaxies in each merging system.

We briefly describe our methods for each of these tasks.

2.1.1 Removing Non-Merging Systems

The examples of Figure 3 demonstrate that the weighted-merger-vote fraction is strongly correlated with how ‘merger-like’ an image appears to be. The outcomes of GZ are therefore similar in effect to automated methods like CAS and GM₂₀ which also map images to parameter spaces. In our case though f_m is a single parameter (making it easier to divide up ‘merger’ and ‘non-merger’ zones) and, by utilising the pattern-recognition capacity of many human minds, overcomes the need to remove background noise, recognise anomalies, etc. We find that for $f_m \gtrsim 0.6$, all systems are robust mergers. However, three causes for mis-classification begin to emerge as f_m decreases and become common for $f_m \lesssim 0.4$:

- (i) projection of **galaxies** along the line of sight,
- (ii) projection of nearby **stars** onto distant galaxies and

⁵ This is the same parent population obtained after six-months of running Galaxy Zoo that is used in Lintott et al. (2008), Land et al. (2008), Bamford et al. (2008a) and Schawinski et al. (2009).

⁶ W here is *not* the w_k of Lintott et al. 2008. w_k is the weighting of each individual user whereas W represents their combined weighting for each individual GZ object.

⁷ This arises because GZ images are scaled for viewing according to the Petrosian radius of the object’s model magnitude. The photometry of very large and close-by galaxies is often deblended into multiple SDSS objects. The more deblended objects there are, the less the Petrosian radius of any single deblended object represents the galaxy as a whole and this brings about an inappropriately small image-scale for viewing some close-by galaxies. Such systems would be viewed by users as nothing but a galaxy core and not, consequently, voted as a merger.

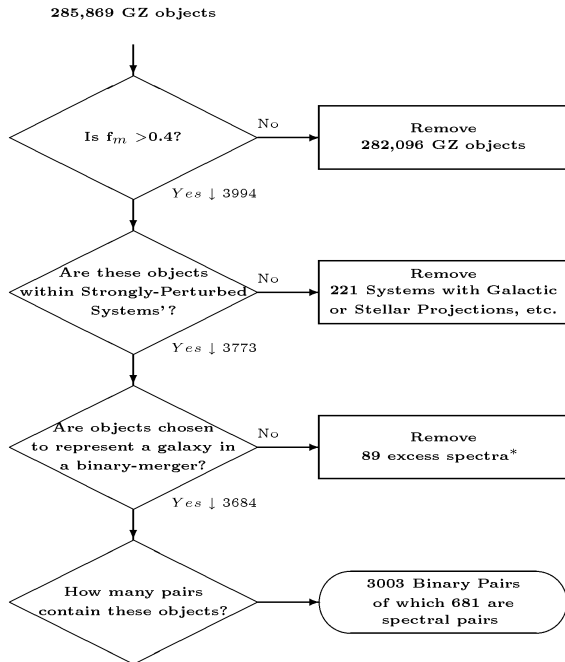


Figure 5. Scheme of binary-merger catalogue production. 285,869 GZ spectral objects lie within $0.005 < z < 0.1$. *89 spectral objects were excluded here because they were in a system where another object was deemed preferable, as in Figure 2.

(iii) cases which are ‘border-line’ mergers.

Galactic projections occur when two galaxies have similar celestial coordinates but are separated by a significant radial distance. We can easily spot projections when *both* galaxies have spectral redshifts. However, many of our candidate systems have only one redshift. Spotting a projection in such cases can only be done through visual examination of the image for signs of interaction. Our choice to use only systems with $f_m > 0.4$ meant, however, that the need for such difficult decisions was rare.

Stellar projections were the more common problem. We were able to eliminate stars easily from our sample though by their characteristic point spread function (PSF) using the associated parameter ‘type’ from the SDSS PhotoTag table. This is a discrete label given to every photometric object in the SDSS database that indicates whether an object is ‘point-like’ or ‘extended’ and can, on this basis, reliably determine (> 98%) whether a luminous object is a star or not (Strauss et al. 2002).

‘Border line’ cases involve galaxies that *are* morphologically disturbed but do not necessarily merit the term ‘merger.’ All galaxies are merging with *something* which can range from molecules (accretion) to a small galaxy (minor merger) to a galaxy roughly its own size (major merger). Deciding where in this spectrum of possibilities the term ‘merger’ becomes appropriate is rather subjective. At this stage, therefore, our strategy was simply to decide by visual inspection whether a given GZ galaxy had a ‘strongly-perturbed’ morphology. By ‘strongly-perturbed’ here we mean that a galaxy was in a morphological state that was unlikely to have occurred without some external inter-

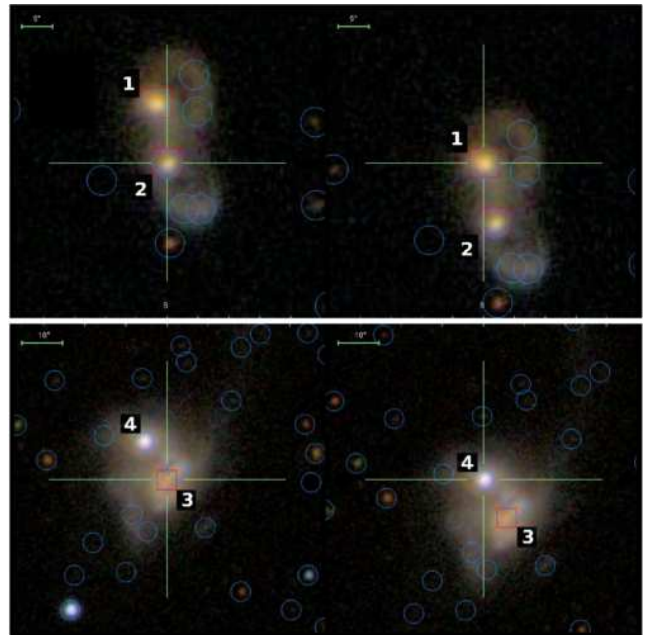


Figure 6. Images exemplifying the construction of the binary merger catalogue. All spectral targets (red boxes) are Galaxy Zoo objects. In the upper panel, we select the two spectral objects (1 and 2) from Galaxy Zoo to represent the merging pair. The merging system in the lower panel only has one spectral target, 3, which was found by Galaxy Zoo. We therefore examine all neighbouring SDSS objects in order to select one (in this case 4) to represent the merging partner galaxy. Our final catalogue has 3003 such pairs.

action. Starting with this inclusive criterion allows us obtain completeness for anything deserving the term ‘merger.’ We found in fact that borderline cases were again rare for systems with $f_m > 0.4$. However, difficult decisions regarding projections and border-line cases are abundant for systems where $0.05 < f_m \lesssim 0.4$ (for example the image of Figure 3 with $f_m = 0.175$) and it will therefore require a great deal of care if we wish to expand our catalogue into the $f_m < 0.4$ range in the future.

We then examine each ‘strongly-perturbed’ system with the aim of selecting an SDSS object to represent the body responsible for the disruption caused to the galaxy labelled with $f_m > 0.4$ (if any is identifiable). The details of this procedure are discussed below. With photometric objects representing the ‘perturber’ we can distinguish major mergers more objectively and their completeness can be assumed since they are a subset of ‘strongly-perturbed’ systems.

In total we removed 221 GZ objects (which were mostly stellar-overlap images) leaving 3773 within actual ‘strongly-perturbed’ systems. The catalogue production is outlined in Figure 5.

2.1.2 Visual Selection of Merging Partner

As mentioned, in order to create a catalogue of *binary* mergers, we sought to manually select an appropriate SDSS object as a partner for the object supplied by GZ with $f_m > 0.4$. We did this using an IDL routine that allows for the rapid examination of the image and photometry of all

objects within $30''$ of the GZ object given by the Neighbors table in the SDSS database. We choose whichever object appears to be the most ‘plausible’ representation of the body responsible for the morphological disruption to the galaxy represented by the GZ object. Plausibility was judged on the basis of object brightness (with brighter objects in the r -band being preferable) and visual ‘common-sense.’ See Figure 6 for examples of this procedure. For most binary mergers this choice was straightforward as they usually have either

- (a) spectra centred on both galaxies,
- (b) a spectral object centred on one galaxy and only photometry on the other or
- (c) only photometry on both.

However, not all ‘strongly-perturbed’ systems appear as simple binary mergers. Additionally, there are cases where

- (d) galaxies are in the final stages of a merger and its progenitors are no longer distinguished by the SDSS pipeline (‘post-mergers’),
- (e) a galaxy has been perturbed by a close encounter with a neighbour no longer in view (‘fly-by’) and, occasionally,
- (f) a merging system involves three or more galaxies.

The wide range of possibilities makes merger taxonomy a difficult task. In constructing a binary-mergers catalogue we therefore proceed as follows for these various cases.

For case (a) we usually choose these two spectral objects to represent our merging pair (see figure 6). On a few occasions, a photometric object was preferred to a spectroscopic object due to its either being brighter or closer to the core and thus a more plausible representation of the galaxy’s luminosity.

If the merger companion does not have spectra then we visually select the best photometric object available to represent the merging partner (case b). In the case of (c) which usually applies to systems where all objects are too faint ($r > 17.77$) to be targeted for spectroscopy the merger would go unnoticed by GZ.

Cases (d) and (e) are sometimes difficult to distinguish and usually occur when only one galaxy core is apparent with the peripheries undergoing extensive tidal disruption. This usually means that no photometric object is available to plausibly represent the perturbing body and so, in such cases, we simply decline to select a merging partner. They remain in the category of ‘strongly-perturbed’ systems but are not included in the binary mergers catalogue. Figure 1 shows examples of this category which account for about 11% of the ‘strongly-perturbed’ systems.

In the case of (f), where several galaxies are merging at once, we decided to first note them and then include them in the binary-mergers catalogue by selecting the closest and brightest object to the GZ-supplied galaxy. Figure 7 shows examples of such systems which comprise about 2% of our binary mergers catalogue.

Through this pairing process we obtain 3003 binary pairs, 681 ($\sim 20\%$) of which are spectral pairs and 78 ($\sim 2\%$) of which are multi-mergers. We refer to these 3003 pairs as

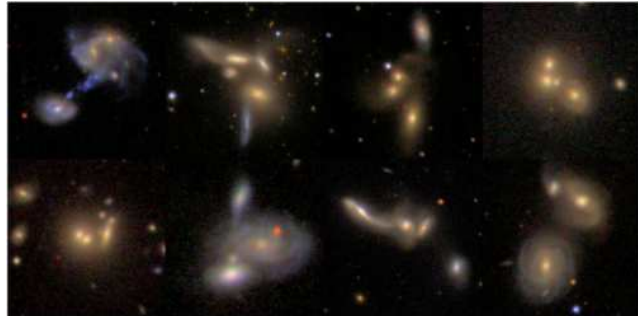


Figure 7. Example images of multi-merging systems. We generally included these in the binary merger catalogue by selecting the closest and brightest galaxy to accompany the Galaxy-Zoo object. We flagged 78 systems in this category which accounts for $\sim 2\%$ of our final catalogue.

our ‘binary-mergers’ catalogue (MGZ1). See Figure 5 for a summary of its construction.

2.1.3 Assigning Morphologies

Morphologies were assigned to each SDSS object in our binary-mergers catalogue by a single classifier (DWD) working with consultation. We use four classifications for the merging galaxies: E, S, EU and SU. The E and S classifications respectively label those galaxies which are clearly elliptical and spiral by morphology. No appeal to colour should be necessary. The EU and SU are those ellipticals and spirals about which we are ‘unsure,’ in other words, this is our best guess.⁸ The ‘unsure’ morphologies are usually more distant objects whose image resolution is too poor to distinguish features like spiral arms. Choosing between EU and SU can be very difficult and is based mostly on apparent surface-brightness profile and, in very difficult cases, on colour. (See Figure 8 for examples and further details of our decision-making criteria.)

A simple means to select morphology in SDSS is via the SDSS *fracdev* parameter measured in the r -band that ranges from 0 to 1. This is a measure of the goodness-of-fit of a galaxy’s surface-brightness to a de Vaucouleur profile. Ellipticals tend to have a *fracdev* ~ 1 whereas spirals have a wide distribution. We find that our morphological categories S, SU, EU and E have mean *fracdev* values of 0.48, 0.85, 0.93 and 0.94 respectively fitting qualitatively with expectation. The high value of 0.85 for the SU category suggests there is contamination by bulge dominated discs or ellipticals as discussed in §3.5. This is expected since distant, poorly-resolved spirals can look like ellipticals (Bamford et al. 2008a). To avoid such contamination we can restrict ourselves at any-time to using only the ‘sure’ morphologies.

3 THE MERGER FRACTION OF THE LOCAL UNIVERSE

Our large binary-mergers catalogue and f_m values given by GZ for 893,292 spectral objects enables us to address two

⁸ We refer to the set of merging galaxies with elliptical classifications as ‘E+EU’ galaxies, etc.

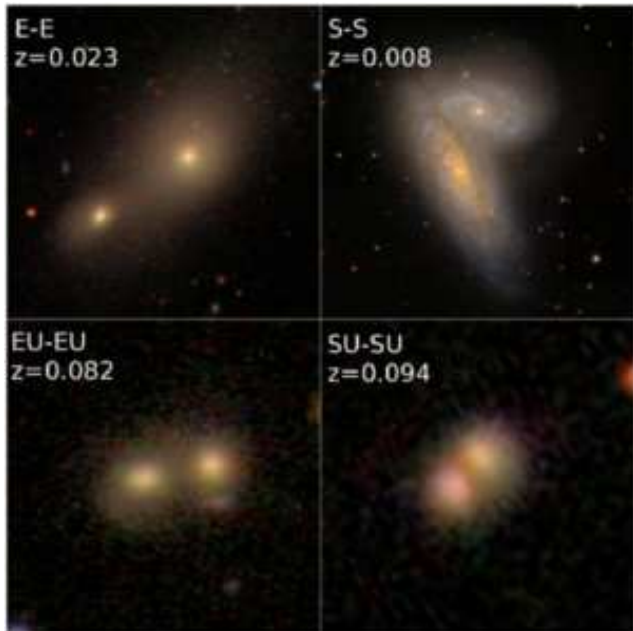


Figure 8. Example images of galaxies for morphological categories E, S, EU & SU. Any combination of these is possible. Poorer image resolution as $z \rightarrow 0.1$ affects certitude of morphological components. The bottom panels show examples of ‘unsure’ morphologies. If a morphology is unclear, it will normally be assigned EU type by surface brightness profile if there is a drop off in brightness from the centre. SU types generally have a more uniform surface brightness profile in our approach. Colour was also used in very difficult cases under the assumption that EU types should be more red.¹⁰

distinct and important questions which are highly relevant to the field of galaxy evolution:

- (i) what is the **fraction** of merging galaxies in the local universe? and
- (ii) what is the **ratio** of spirals to ellipticals (N_s/N_e) in mergers in the local universe?

Our binary mergers catalogue, while large, is incomplete since it is constructed only from systems with $f_m > 0.4$. Answering either of these questions will therefore require extrapolation into the $0 < f_m < 0.4$ region. Throughout this study, we define a major merger to be two merging galaxies of stellar masses M_1 and M_2 where $1/3 < M_1^*/M_2^* < 3$.

3.1 Estimating the Merger Fraction (I)

Our merger location technique is different to those before it and is suited therefore to a different procedure for finding a meaningful ‘merger fraction’ which we make explicit here. Our primary goal is to find the fraction of volume-limited galaxies in the local universe currently undergoing a *major merger* since these are thought to drive the morphological mix of the universe following the work of Toomre & Toomre (1972). To find this though we need to separate major from minor mergers. To do this we first estimate the fraction of ‘strongly-perturbed’ galaxies in the universe using GZ data. We will then want to know what subset of these ‘strongly-perturbed’ galaxies are in major mergers. This second part

shall be carried out once we have stellar mass estimates for the 3003 pairs in our binary-merger catalogue (§3.2).

To accomplish the first task of estimating the fraction of ‘strongly-perturbed’ galaxies in the local universe we use the subset of our GZ spectral objects that are members of the Main-Galaxy-Spectral sample (MGS; Strauss et al. 2002) in SDSS to find:

$$f_{mgs} = \frac{\sum \left[\begin{array}{c} \text{‘Strongly-perturbed’ volume-limited} \\ \text{MGS spectral objects in SDSS} \end{array} \right]}{\sum \left[\begin{array}{c} \text{All volume-limited} \\ \text{MGS spectral objects in SDSS} \end{array} \right]}. \quad (2)$$

The use of only those spectral objects which are in the MGS leads to a good approximation for the *real* merger fraction, f_{real} where $f_{real} = C f_{mgs}$ with the correction factor $C \sim 1.5$). Justification for this claim with a brief discussion of the MGS and spectroscopic targeting in SDSS is outlined in Appendix A.

To find the numerator of (2), we took volume-limited samples of 100 GZ-spectral objects from the bins $0 < f_m \leq 0.05$, $0.05 < f_m \leq 0.20$ and $0.20 < f_m \leq 0.40$ which are also in the MGS. By visually inspecting each set of 100 galaxies *twice* (the first time round we made our decisions very conservatively, the second time round very liberally) we obtained estimates for the percentages of ‘strongly-perturbed’ galaxies within our stated ranges. These were: 0 – 2%, 18 – 34% and 50 – 59% for the $0 < f_m \leq 0.05$, $0.05 < f_m \leq 0.20$ and $0.20 < f_m \leq 0.40$ bins respectively. There are, of course, many more objects in these bins than in those with $f_m > 0.4$ (see Figure 4) and so end up contributing to at least two thirds of all ‘strongly-perturbed’ systems. We assumed that no GZ object with $f_m = 0$ would be ‘strongly-perturbed.’

Applying these estimated fractions to the total number of MGS objects in each bin and adding the ‘strongly-perturbed’ and volume-limited MGS objects from our $f_m > 0.4$ catalogue gives us the numerator for equation (2) and hence the fraction f_{mgs} . We sum up our result in the following way:

The Merger Fraction (Weak Statement)
 $\sim 4 - 6\%$ of all galaxies with $M_r < -20.55$ in the local universe ($0.005 < z < 0.1$) are ‘strongly-perturbed.’

We call this the weak statement because of the subjective nature of deciding whether or not a system is ‘strongly-perturbed’ or not. The error in this percentage arises from the upper and lower bounds estimated for the three samples of 100 images. As mentioned, in §3.3 we estimate the fractions of our 3003 catalogue-pairs that constitute major mergers and use these plus a few more plausible assumptions to offer a stronger statement for the major-merger fraction in the local universe.

We also double checked our results with an additional interface on the world-wide web designed to re-examine all objects within the range $0.2 < f_m < 0.4$. We found that this corroborated our estimate that 50 – 59% of galaxies in this range are ‘strongly-perturbed.’ See Appendix B for details.

3.2 The Stellar Masses of Merging Galaxies

We measure the stellar masses for each binary pair by fitting the SDSS photometry to a library of photometries produced

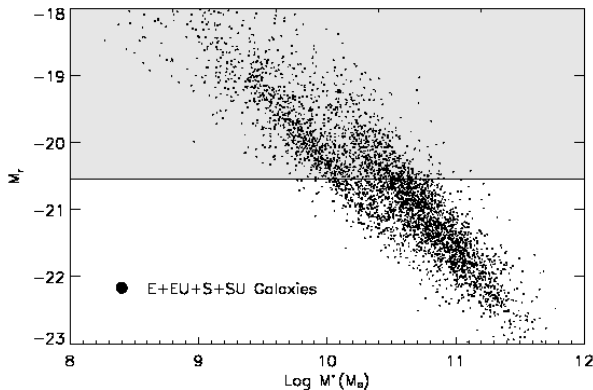


Figure 9. Relation between stellar mass and absolute magnitude in the r -band. The solid horizontal line at $M_r = -20.55$ corresponds to the cut used to obtain our volume-limited samples. This cut removes virtually all galaxies with mass $M < 10^{10} M_\odot$ as well as galaxies up to a mass of $M \sim 7 \times 10^{10} M_\odot$.

by a variety of two-component star formation histories. The approach is similar to that of Schawinski et al. (2007a) except that we do not use the information contained in the stellar absorption indices. The library SEDs are generated using the Maraston (1998, 2005) stellar models. Both components have stellar populations with variable age with fixed solar metallicity and Salpeter IMF (Scarlata et al. 1955). The first (older) burst is a simple stellar population (SSP), the second (more recent) burst is modelled by an exponential with variable e-folding time. The purpose of the varying e-folding times is to account for galaxies with extended star formation histories. This is especially important for mergers which are likely to have undergone recent star-formation episodes. Dust is implemented using a Calzetti et al. law (Calzetti 2000) that is free to vary for $E(B-V)$ over 0 to 0.6. It should be noted that mergers, by their very nature, are prone to mix and overlap and this could lead to additional reddening. In D09b we examine the distributions of these stellar masses in more detail and in comparison to a control sample.

It is important that our cut for the merger fraction be based upon magnitude and not mass since it is the photometric brightness of the object that determines whether or not it will end up in the MGS (which is integral to our definition of the merger fraction). In Figure 9 we examine the effect of imposing our volume-limiting cut on the mass distributions. Mass scales with brightness though the scatter is substantial such that the magnitude limit $M_r < -20.55$ removes all galaxies with $< 10^{10} M_\odot$ and some as massive as $\sim 7 \times 10^{10} M_\odot$. In order to estimate the merger fraction using a mass cut (instead of a magnitude cut) for this redshift range, one would therefore need to make it no less than $\sim 7 \times 10^{10} M_\odot$ to ensure completeness. Practically, in order to calculate the merger fraction, we would need masses for the entire MGS sample to get the denominator of 2. This is not an easy computational task.

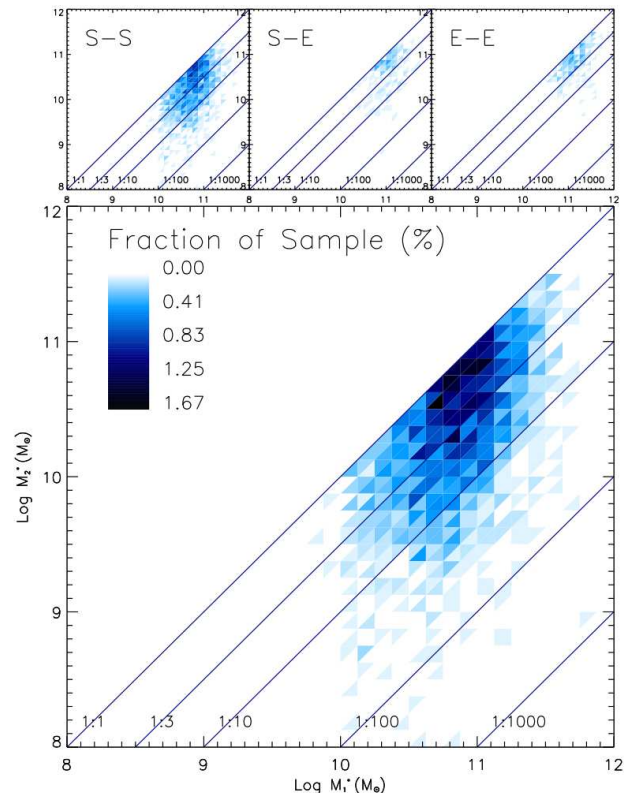


Figure 10. This figure illustrates the occupancy of regions in mass-mass space for all binary mergers where the *more massive* galaxy has $M_r < -20.55$. This sample has 1963 mergers. 1031 ($\sim 53\%$) are within the ‘major-merger’ strip ($M_1^*/M_2^* < 3$).

3.3 Estimating the Merger Fraction (II)

Figure 10 illustrates the occupation of the mass space of our mergers with the magnitude limit imposed on the *more massive* galaxy in the pair (i.e. a point will be included if the magnitude of the more massive galaxy has $M_r < -20.55$, regardless of the brightness of the companion). This criterion allows us to view both major and minor mergers. We find that $\sim 50\%$ of these points lie within the major-merger strip. Estimation of the number of minor mergers within our volume-limited ranges is difficult since their completeness rapidly diminishes as M_1^*/M_2^* increases.

Knowledge of the stellar-masses thus allows us to estimate what subset of the ‘strongly-perturbed’ MGS spectral objects in the local universe which we found in §3.1 are major mergers. Of the 3864 spectral objects in our 3003 binary-merger pairs, 2306 have $M_r < -20.55$. Of these, 1243 are in major mergers leaving 1063 in minor mergers. We therefore have $1243/2306 \sim 54\%$ of our volume-limited spectral objects in major mergers.

We can estimate an upper-limit for the fraction of major mergers now by supposing that this fraction of major mergers from what was originally classified as a set of ‘strongly-perturbed’ systems will be the same for *all* strongly-perturbed systems - even in the range $f_m < 0.4$. This is certain to be an *overestimate* since there are bound to be a higher portion of major mergers in systems with high f_m . The reason for this is that most ‘strongly-perturbed’ systems obtain a low $f_m \sim 0.2$ precisely because they are

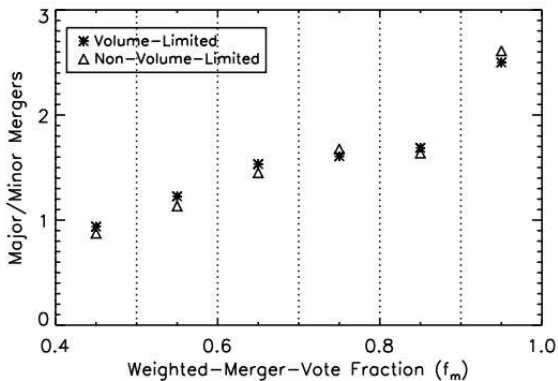


Figure 11. The relationship of major-to-minor-mergers ratio for the binary-mergers catalogue over the $0.4 < f_m < 1.0$ range. The trend indicates that major mergers are more likely to get merger votes than minor mergers. Minor mergers only outnumber major mergers in the $0.4 < f_m < 0.5$ bin. The effect is similar for both volume- and non-volume limited samples.

mostly ‘border-line’ cases (i.e. perturbations caused by interactions or very minor mergers). Figure 11 confirms this expected relationship over the range of f_m for our catalogue, that is, the fraction of major-to-minor mergers in our sample is seen to increase with f_m . In other words, users more readily identified equal mass mergers on average. Applying this fraction of 54% to the upper limit of our weak statement gives $0.54 \times 6\% = 3.24\%$ which, being an overestimate, we can plausibly round down to $\sim 3\%$.

We can also obtain a lower-limit to the major-merger fraction by supposing that the major mergers in our catalogue comprise *all* of the major mergers in the local universe. That is, we can suppose that there are no major mergers at all in the range $f_m < 0.4$ for our volume-limited sample. This is of course an *underestimate* since there are bound to be at least some major mergers in, for example, the range $0.2 < f_m < 0.4$. Nonetheless, applying this assumption gives the lower limit of $1243/157,801 \sim 0.8\%$. Again, since this is undoubtedly an underestimate, we can plausibly round this limit up to $\sim 1\%$. We summarise this working in the following way.

The Merger Fraction (Strong Statement)

$\sim 1 - 3\%$ of all galaxies with $M_r < -20.55$ in the local universe ($0.005 < z < 0.1$) are observed in a major merger.¹¹

3.4 Close Pairs Comparison

Comparing this fraction with close-pairs studies is difficult because few of them present their results in terms of merger fractions. They also use different criteria for their volume-limiting bounds and for accounting for errors which are important in such studies (such as fiber collisions, false-pairs and non-gravitationally bound pairs). For example, Patton et al. (2000) concluded that $\sim 1.1\%$ of nearby galaxies with $-21 < M_B < -18$ are undergoing a merger (but not

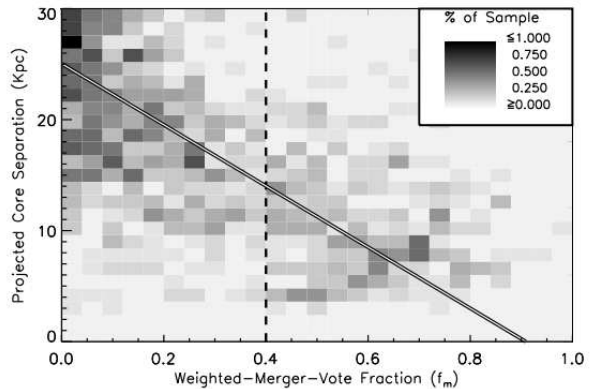


Figure 12. The distribution of volume-limited close-pairs objects in the MGS comparing f_m and their projected separations. The vertical broken line marks the boundary for our merger catalogue at $f_m = 0.4$. The solid diagonal line is a best-fit to the distribution of points in this f_m -separation space. The shading indicates the density of points in various regions of this space. GZ users were more likely to call a close-pairs object a merger as the projected core-separation decreased.

necessarily a *major* merger by our definition). Our percentage is similar but the definitions are so diverse as to render comparison obsolete.

A more recent study by Patton et al. (2008) on SDSS close-pairs measures the number of ‘close-companions’ per spectral object which satisfy three constraints: physical separation (r_p ; $5 < r_p < 20h^{-1}$), rest-frame velocity ($\Delta v < 500\text{kms}^{-1}$) and absolute magnitude difference ($|\Delta M_r| \leq 0.753$). Again though, there are significant differences between their samples and ours. Their magnitude limits are $-22 < M_r < -18$ and they define a major merger by magnitude (at 1:2 luminosity), not by mass as we do (at 1:3). More significantly, only \sim half of the pairs satisfying their criteria are “known to exhibit morphological signs of interactions” whereas our sample is selected on the basis of visually-established interactions. So although the number of close-companions they calculate, $N_c \sim 0.02$, is similar to our major-merger fraction, $\sim 1-3\%$, the differences between the two techniques make claims of corroboration difficult to substantiate.

We performed our own comparison of GZ with a close-pairs catalogue of all SDSS spectral objects within a projected separation of 30kpc of each other and a line-of-sight velocity difference of $< 500\text{kms}^{-1}$. For a consistent comparison with our catalogued mergers, we examine only those objects which are within the volume-limited boundaries ($0.005 < z < 0.1$; $M_r < -20.55$) and the MGS. This gives 2308 individual close-pair objects. Many of these will be part of a false-pair arising from the automated deblending of a single galaxy into two or more spectral targets. Some pairs will also appear well separated (relative to their size) and show no signs of interaction. We therefore visually examined all 2308 objects in order to determine which ones are in a ‘strongly-perturbed’ state brought about by the other spectral object in the pair. This led to the removal of 654 ($\sim 28\%$) of the close-pairs objects in our volume-limited MGS sample.

The 1654 remaining spectral objects are all GZ objects

¹¹ We omit the corrective factor $C \sim 1.5$ here since it is of order unity and the fraction is already given as an approximation.

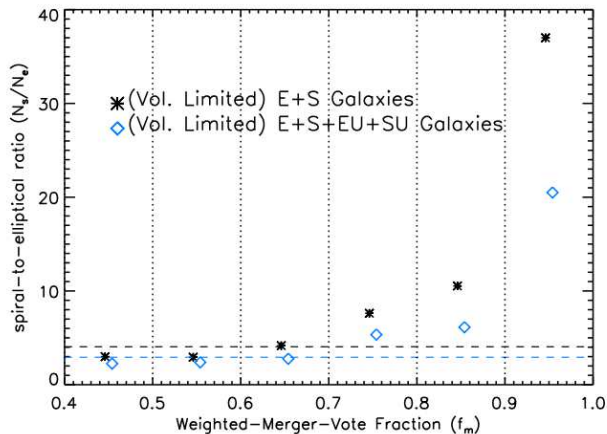


Figure 13. An examination of the relation between morphology and f_m (here as %). We magnitude limit our sample ($M_r < -20.55$) and measure the ratios of spiral to elliptical morphologies (N_s/N_e) of mergers for bins shown along the f_m axis. As $f_m \rightarrow 1.0$ a strong bias is seen for users to flag mergers involving spirals. N_s/N_e appears to converge to roughly a constant as $f_m \rightarrow 0.4$. The broken horizontal lines are the mean N_s/N_e values for the two samples over the whole range $0.4 < f_m \leq 1.0$.

and so we can examine how users voted for them. We found that a significant portion ($\sim 64\%$) of these close-pair spectral objects which are in ‘strongly-perturbed’ systems (by our reckoning) had $f_m < 0.4$ and were therefore excluded from our catalogue. However, we also found that there is a strong correlation between f_m for close-pair objects and their *projected separation* such that the further apart close-pair objects are, the less likely users were to label it a merger (see Figure 12). This means that the GZ technique selects systems which are generally more advanced in the merger process and therefore undergoing more extensive interactions than a typical system in close-pairs studies. Only ~ 600 of these objects are in our catalogue of ~ 3000 pairs which fits with the claim that only $\sim 20\%$ of (relatively advanced) merging systems are spectral pairs in SDSS, the rest being systems with only a single spectral object within our magnitude-limited volume.

3.5 Estimating the Spiral to Elliptical Ratio in Merging Systems

3.5.1 Uncertainties and User Bias

A more difficult task is to estimate the spiral-to-elliptical ratio of galaxies that are merging (N_s/N_e) where N_s and N_e are the number of galaxies in the binary-mergers catalogue that are spiral and elliptical respectively. In addition to the uncertainties associated with identifying actual mergers, there are the uncertainties associated with varying image resolution leading to ‘sure’ and ‘unsure’ morphologies. Bamford et al. (2008a) have studied extensively the dependence of GZ morphological classifications on redshift and found that the proportion of elliptical classifications increases with z . The same problem arose for our classifications: over the range $0.005 < z < 0.03$ the fraction of ‘unsure’ morphologies (EU, SU) to ‘sure’ morphologies (E, S) is $< 10\%$ but this fraction rises to $\sim 25\%$ as we vary over

$0.03 \rightarrow 0.1$. In short, the more distant a galaxy is the more ‘featureless’ it appears bringing about a visual misclassification that inflates the recorded number of ellipticals. (For details of the quantification and correction to this effect, see Bamford et al. (2008a).)

A further unknown peculiar to GZ is mass-user psychology. A natural concern of ours was that users would be more likely to call a system a ‘merger’ if it involves two spirals (which generally look more dramatic) than if it involves two ellipticals. We therefore examine how the ratio of spirals to ellipticals in our volume-limited binary mergers catalogue varies with f_m as shown in Figure 13. Whether we use just the ‘sure’ morphologies (E+S sets) or whether we include the ‘unsure’ morphologies (E+S+EU+SU sets), the N_s/N_e ratios appear to follow curves that start high for $f_m \sim 1.0$ and decay towards a constant as $f_m \rightarrow 0.4$. This confirmed the suspicion that the systems compelling users to click the merger button the most tend to involve spirals. However, the majority of mergers are located in the bins where the ratios level off at roughly a constant. Inclusion of the EU and SU categories slightly decreases N_s/N_e as expected (some ‘unsures’ are really spirals but get mistaken for ellipticals).

The horizontal lines of Figure 13 indicate the mean N_s/N_e ratios for the E+S and E+S+EU+SU samples over the whole range $0.4 < f_m < 1.0$. These N_s/N_e means are ~ 5 and ~ 3 respectively. The true mean over this range must surely be $\langle N_s/N_e \rangle > 3$ therefore since the ‘unsure’ morphological categories deflate N_s/N_e through false inclusion of ellipticals as discussed earlier.

3.5.2 Towards an N_s/N_e Estimate for Merging Galaxies

We proceed now by extrapolating this value $N_s/N_e > 3$ (found for the range $f_m > 0.4$) to the entire range of f_m , that is, we assume $N_s/N_e > 3$ for all galaxies in mergers for our volume-limited ranges. We compare this ratio with the global spiral-to-elliptical ratio for all galaxies in our redshift range determined using the corrections of Bamford et al. (2008a) to debias the high occurrence of ellipticals with increasing redshift. This debiasing leads to the estimate that there are $\sim 1.5/1$ spirals to ellipticals for all galaxies with $M_r < -20.55$ in our redshift range. Our extrapolated estimate of $N_s/N_e > 3$ for $f_m > 0.4$ is significantly higher in comparison, i.e. our extrapolation would suggest that spirals feature in mergers roughly twice as often as they should if selected randomly from the global population.

To test the accuracy of this extrapolation we examined the morphologies of the same 59 systems from the 100 images of $0.2 < f_m < 0.4$ (used in §3.1) that were deemed to be ‘strongly-perturbed.’ We found that 42/59 of these ‘strongly-perturbed’ galaxies were either S or SU and the remaining E or EU. Taking $N_s/N_e \sim 1.5$ for the global estimate to give null binomial probabilities $p(\text{spiral}) = 0.6$ and $p(\text{elliptical}) = 0.4$, the expected outcome of 59 galaxy morphologies would be $35.4 \pm \sigma$ spirals with standard deviation $\sigma \sim 3.8$. The observed number, 42, is just within two standard deviations of the expected value. This observation therefore supports the claim that, even in the range $0.2 < f_m < 0.4$, N_s/N_e in mergers is higher than the global mean. This also does not take into account the fact that our observations are still biased by inclusion of ‘unsure’ morphologies (which inflates the number of ellipticals) whereas

the estimate $N_s/N_e \sim 1.5$ for the global population has been debiased.

To summarise, we find that $N_s/N_e > 3$ over the range of our binary mergers catalogue ($f_m > 0.4$). This is at least twice the global ratio ($N_s/N_e \sim 1.5$). There is no evidence to suggest that mergers in the range $f_m < 0.4$ will compensate this effect with an excess of ellipticals relative to their global population. The high N_s/N_e ratio is especially likely to stand up to scrutiny for *major*-mergers since they have been shown to favour higher values of f_m (see Figure 11) where the spiral excess has been robustly confirmed.

3.5.3 Implications of a High N_s/N_e Ratio in Mergers

We now discuss possible reasons for a high N_s/N_e ratio in mergers. It is well established that spirals tend to occupy less-dense environments than ellipticals (verified as early as Oemler 1974 and as well as recently, e.g. Ball et al. 2008). The discrepancy might therefore be the result of a preference for mergers to occur in field environments where spirals are more populous relative to the global population. Alternatively though, the disproportionate number of spirals in our ‘snapshot’ of the local universe could indicate that the time-scales over which spiral galaxies remain detectable in mergers exceeds that of ellipticals.

Studies have been carried out to estimate the time-scales of mergers using dynamical-friction arguments (e.g. Conselice 2006a) and simulations (e.g. Bell et al. 2006; Conselice 2006a; Lotz et al. 2008b). Lotz et al. (2008b), in particular, focus on this question and find that the gas-fraction of galaxies in mergers is one of several factors determining the time-scale of detectability. One such simulation comparing two equal-mass mergers with different gas-fractions showed that the system with the higher gas-fraction ($f_{gas} \sim 50\%$) remained ‘morphologically disturbed’ (i.e. flagged as a merger by the standard criteria of G, M₂₀, C, A combinations) for 2 – 4 times longer than the system with a lower gas-fraction ($f_{gas} \sim 20\%$).

In practise, any variation in N_s/N_e for merging galaxies will depend on a combination of these two explanations since, *a priori*, it seems certain that the merger frequency will have some dependence on environment and the merger-time-scale detectability some dependence on the internal characteristics that distinguish spirals from ellipticals such as gas-content and overall mass. We examine these two effects in detail in the companion paper D09b.

4 SUMMARY AND DISCUSSION

Galaxy Zoo is a new and powerful strategy for locating mergers. The technique is similar in its effect to the CAS and GM₂₀ methods in that it converts images to numbers that provide a measure of how ‘merger-like’ a galaxy is (in this case the weighted-merger-vote fraction $f_m \in [0, 1]$). The method is highly robust because f_m is the averaged product of human minds (which are highly adept at pattern recognition) and is therefore extremely sensitive to details while doing away with the major programming challenges associated with automated methods. It is also easier to partition merger-spaces in this method since f_m is a single parameter unlike CAS and GM₂₀ which demand more fine-tuning. The

technique is also not limited to objects with spectra as the close-pairs method is (by definition) and we find in fact that only $\sim 20\%$ of our merging systems have spectra on both galaxies. This is mostly due to the large fraction of the SDSS sky that suffers from fiber-collisions ($\sim 70\%$; Strauss et al. 2002, Blanton et al. 2003). It also means that the method is effective at the broader task of finding ‘strongly-perturbed’ systems including minor mergers. The drawbacks to GZ are time and repeatability. The results presented in this paper are derived from about six months of active web activity.

It is worth emphasising that the results of this paper are entirely derived from the pressing of a single button labelled ‘merger.’ The simplicity of this interface lead to an unfortunate dichotomy whereby users were often unsure whether to emphasise the merger aspect or the morphological aspect of a given system. Now that the competence and eagerness of the public to assist in extragalactic astronomy is known and tested, we expect greatly improved results with the Galaxy Zoo 2 project - a new development that will enable finer classification of SDSS objects as well as higher redshift surveys.

Galaxy Zoo has already yielded rich results with the initial merger catalogue presented here containing 3003 robust binary mergers in the range $0.005 < z < 0.1$ created from GZ objects with $f_m > 0.4$. Each has been visually-inspected by fifty or so Galaxy-Zoo users and by one of the authors (DWD). We believe that it is the largest of its kind. Completeness, however, remains an issue as users and experts are only as accurate as the image quality allows. As redshift increases, the reduced image quality makes it difficult to identify galactic projections. Also, there will always be the problem for any merger-detection method in deciding whether or not a galaxy perturbation (such as an extended tidal tail) is great enough to warrant the term ‘merger.’ For these two reasons, there is a large number of ‘border-line’ cases in the range $0 < f_m < 0.4$ which are responsible for the error in our estimate of the merger fraction in the local universe.

To obtain this merger fraction, we first estimated the number of ‘strongly-perturbed’ galaxies with spectra in bins over the range $0 < f_m < 0.4$ plus those in our catalogue. Dividing this number by the total number of volume-limited spectral objects lead us to estimate that 4 – 6% of all such galaxies ($0.005 < z < 0.1$ and $M_r < -20.55$) are ‘strongly-perturbed.’ We expanded upon this statement by estimating what subset of ‘strongly-perturbed’ volume-limited spectral galaxy objects are involved in major mergers in the local universe. This led to the stronger statement that:

$\sim 1 - 3\%$ of volume-limited galaxies in the local universe ($M_r < -20.55, 0.005 < f_m < 0.1$) are observed in major mergers.¹²

We also estimated the ratio of spirals to ellipticals for merging galaxies with $M_r < -20.55$. The N_s/N_e ratio for our catalogue was highly in favour of spirals by about 3/1. We examined 100 systems in the range $0.2 < f_m < 0.4$ and found a similar number. This is large compared to the global N_s/N_e ratio ($\sim 1.5/1$) for this magnitude-limited volume. We therefore concluded that more spirals are seen to be

¹² This fraction also requires a correction factor close to unity. In Appendix A we estimate it to be $C \sim 1.3$.

merging than ellipticals, perhaps by as much as factor ~ 2 . We then discussed possible reasons for this observed spiral excess suggesting that either (1) mergers tend to occupy environments that favour spirals, or (2) the time-scale for a merger to reach a relaxed state (i.e. the time over which it is detectable) is longer for spirals than for ellipticals.

The probability, p_o , of observing a galaxy merging at any general time is proportional to the probability of its merging at that time, p_m , multiplied by the time-scale, τ , over which it is detectable, $p_o \propto p_m \tau$. The probability of merging should only depend on the system's mass and environment ($p_m = p_m(M, \rho)$) whereas the time-scale of detectability, τ , must be assumed *a priori* to depend on the internal properties of the merging galaxy such as gas content and mass distribution. Our high N_s/N_e ratio therefore suggests that either $p_m(M, \rho)$ or τ is large for spirals compared to ellipticals.

We disentangle these effects in the companion paper D09b by exploring the role of the environment and the internal properties of this merger sample. We find in fact that mergers occupy the same (if not slightly *denser*) environments as a randomly selected control sample of galaxies. We conclude therefore that the best explanation of an apparently high spiral-to-elliptical ratio in mergers, as we find here, must be due to varying time scales of detectability. The properties of spirals and ellipticals that affect detectability are therefore an important issue that the Galaxy Zoo catalogue can help us understand.

5 ACKNOWLEDGMENTS

D. W. Darg acknowledges funding from the John Templeton Foundation. S. Kaviraj acknowledges a Research Fellowship from the Royal Commission for the Exhibition of 1851 (from Oct 2008), a Leverhulme Early-Career Fellowship (till Oct 2008), a Senior Research Fellowship from Worcester College, Oxford and support from the BIPAC institute, Oxford. C. J. Lintott acknowledges funding from The Levehulme Trust and the STFC Science in Society Program. K. Schawinski was supported by the Henry Skynner Junior Research Fellowship at Balliol College, Oxford.

Funding for the SDSS and SDSS-II has been provided by the Alfred P. Sloan Foundation, the Participating Institutions, the National Science Foundation, the U.S. Department of Energy, the National Aeronautics and Space Administration, the Japanese Monbukagakusho, the Max Planck Society, and the Higher Education Funding Council for England. The SDSS Web Site is <http://www.sdss.org/>. The SDSS is managed by the Astrophysical Research Consortium for the Participating Institutions. The Participating Institutions are the American Museum of Natural History, Astrophysical Institute Potsdam, University of Basel, University of Cambridge, Case Western Reserve University, University of Chicago, Drexel University, Fermilab, the Institute for Advanced Study, the Japan Participation Group, Johns Hopkins University, the Joint Institute for Nuclear Astrophysics, the Kavli Institute for Particle Astrophysics and Cosmology, the Korean Scientist Group, the Chinese Academy of Sciences (LAMOST), Los Alamos National Laboratory, the Max-Planck-Institute for Astronomy (MPIA), the Max-Planck-Institute for Astrophysics (MPA),

New Mexico State University, Ohio State University, University of Pittsburgh, University of Portsmouth, Princeton University, the United States Naval Observatory, and the University of Washington.

REFERENCES

- Abraham R. G., van den Bergh S., Nair P., et al., 2003, *ApJ*, 588, 218A.
- Ball N. M., Loveday J., Fukugita N. M., Nakamura O., Okamura S., Brinkmann J., Brunner R. J., 2008, *MNRAS*, 348, 1038.
- Ball N. M., Loveday J., Brunner R. J., 2008, *MNRAS*, 383, 907B.
- Bamford S. P. et al., 2008, submitted to *MNRAS*, arXiv:0805.2612.
- Barton E. J., Arnold J. A., Zentner A. R., Bullock J. S., Wechsler R. H., 2007, *AJ*, 671, 1538.
- Bell E. F., Phleps S., Somerville R. S., Wolf C., Borch A., Meisenheimer K., 2006, *ApJ*, 652, 270B.
- Bernardi M., et al., 2003, *AJ*, 125, 1817B.
- Blanton M. R., Lin H., Lupton R. H., Maley F. M., Young N., Zehavi I., Loveday J., 2003, *AJ*, 125, 2276.
- Bond J. R., Cole S., Efstathiou G., Kaiser N., 1991, *ApJ*, 379, 440.
- Bundy K., Ellis R. S., Conselice C. J., 2005, *AJ*, 625, 621.
- Calzetti D., Armus L., Bohlin R. C., Kinney A. L., Koornneef J., Storchi-Bergmann T., *ApJ*, 533, 682.
- Capak P., Abraham R. G., Ellis R. S., Mobasher B., Scoville N., Sheth K., Koekemoer A., 2007, *ApJS*, 172, 284.
- Carlberg R. G. et al., 2000, *ApJ*, 532, 1.
- Cole S., Lacey C. G., Baugh C. M., Frenk C. S., 2000, *MNRAS*, 319, 168.
- Conselice C. J., 2003a, *ApJS*, 147, 1
- Conselice C. J., Bershady M. A., Dickinson M., Papovich C., 2003b, *ApJS*, 126, 1183.
- Conselice C. J., 2006, arXiv:0610662v2
- Conselice C. J., 2006, *AJ*, 638, 686
- Conselice C. J., Rajgor S., Myers R., 2008, arXiv:0711.2333v1
- Cox T. J., Jonsson P., Somerville R. S., Primack J. R., Dekel A., 2008, *MNRAS*, 384, 386
- Darg D. W. et al., 2009, *MNRAS*, submitted (D09b in paper)
- De Lucia G., Springel V., White S. D. M., Croton D., Kauffmann G., 2006, *MNRAS*, 366, 499
- Di Matteo T., Springel V., Hernquist L., 2005, *Nature*, 433, 604
- Dressler A., 1980, *AJ*, 236, 351
- Ellison S. L., Patton D. R., Simard L., McConnachie A. W., 2008, *AJ*, 135, 1877
- Fakhouri O., Ma C.-P., 2008, *MNRAS*, 386, 577
- Fukugita M. et al., 2007, *AJ*, 134, 579
- Hopkins A. M. et al., 2003, *ApJ*, 599, 971
- Hopkins P. F., Cox T. J., Younger J. D., Hernquist L., 2009, *ApJ*, 691, 1168
- B. C. Hsieh, H. K. C. Yee, H. Lin, M. D. Gladders, D. G. Gilbank, 2008, *ApJ*, 683., 33H
- Jogee S. et al., 2008, arXiv:0802.3901
- Jogee S., 2008, arXiv:0408383v2
- Kaviraj S., 2007, arXiv:0801.0127v1

Kaviraj S., 2007, arXiv:0710.1311v1
 Keel W. C., Kennicutt R. C. Jr., Hummel E., van der Hulst J. M., 1985, AJ, 90, 708
 Kennicutt R. C. Jr., Roettiger K. A., Keel W. C., van der Hulst J. M., Hummel E., 1987, AJ, 93, 1011
 Khochfar S. & Burkert A., 2003, AJ, 597, 117
 Lacey C. & Cole S., 1993, MNRAS, 262, 627
 Lahav O., Naim A., Sodre L. Jr., Storrie-Lombardi M. C., 1996, MNRAS, 283, 207
 Land K. et al., 2008, MNRAS, 388, 1686L
 Le Fevre O. et al., 2000, MNRAS, 311, 565
 Li C., Kauffmann G., Heckman T. M., White S. D. M., Jing Y. P., 2008, MNRAS, 385, 1915
 Lin L. et al., 2008, ApJ, 681, 232L
 Lintott C. J. et al., 2008, MNRAS, 389, 1179L
 Lisker T., 2008, ApJS, 179, 319L
 Lotz J. M., Primack J. & Madau P., 2004, AAS, 36, 1615
 Lotz J. M. et al., 2008, ApJ, 672, 177
 Lotz J. M., Jonsson P., Cox T. J., Primack J. R., 2008, MNRAS, 391, 1137L
 Nakamura O., Fukugita M., Yasuda N., Loveday J., Brinkmann J., Schneider D. P., Shimasaku K., SubbaRao M., 2003, AJ, 125, 1682
 Oemler A., 1974, ApJ, 194, 1
 Park C., Choi Y.-Y., Vogeley M. S., Gott J. R. III, Blanton M. R., 2007, ApJ, 658, 898
 Patton D. R., Carlberg R. G., Marzke R. O., Pritchett C. J., da Costa L. N., Pellegrini P. S., 2000, ApJ, 536, 153
 Patton, D. R. et al., 2002, ApJ, 565, 208P
 Patton, D. R. & Atfield J. E., 2008, ApJ, 685, 235P
 Salpeter E., 1955, ApJ, 121, 161
 Scarlata C. et al., 2007, ApJS, 172, 406
 Schawinski K., Thomas D., Sarzi M., Maraston C., Kaviraj S., Joo S.-J., Yi S. K., Silk J., 2007a, MNRAS, 382, 1415
 Schawinski K. et al., 2009, (in preparation)
 Schweizer F., 2005, ASSL, 329, 143S
 Skibba R. A., Bamford S. P., Nichol R. C., Lintott C. J., et al., 2008, MNRAS, submitted
 Slosar A. et al., 2009, MNRAS, 392, 1225S
 Stoughton C. et al., 2002, AJ, 123, 485
 Strauss M. A. et al., 2002, AJ, 124, 1810
 Toomre A. & Toomre J., 1972, ApJ, 178, 623
 Van der Wel, A., 2008, ApJ, 13, 675
 White S. D. M. & Rees M. J., 1978, MNRAS, 183, 341
 Woods D. F. & Geller M. J., 2007, AJ, 134, 527
 York D. G. et al., 2000, AJ, 120, 1579

APPENDIX A: ESTIMATING THE MERGER FRACTION USING SPECTRAL OBJECTS

Here we clarify some of the subtle issues that arise when attempting to estimate the merger fraction of the universe. It was claimed in §3.1 that one could use spectral objects alone to obtain an accurate estimate of the merger fraction. This is true even though a sizable number of galaxies in the universe are strongly-perturbed but do not have spectra due to fiber collisions preventing two spectral targets within $55''$ from both obtaining spectra in regions with only a single tiling. In overlap regions, there is near spectral completeness for spectral targets (Strauss et al. 2002; Blanton et al. 2003).

Firstly, in calculating the merger fraction, we only

use spectral objects belonging to the Main-Galaxy-Spectroscopic sample (MGS) in SDSS. This is the collection of targets identified photometrically as galaxies (but not quasars or luminous red-galaxies; Stoughton et al. 2002; Strauss et al. 2002) with $r < 17.77$ and is intended for statistical sampling of galaxies from a uniform population (Strauss et al. 2002).

Figure A1 depicts a simple tiling scheme analogous to that employed by SDSS (Blanton et al. 2003). The shaded area represents the overlap which we say covers a fraction k_{sky} of the tiled area (for SDSS $k_{sky} \sim 30\%$). Two objects within $55''$ in non-overlap regions suffer from fiber-collision so that only one can get measured. Within overlap regions virtually all targets get measured due to multiple tiling opportunities. Altogether about 6% of all MGS targets do not obtain spectral measurements due to fiber collisions (Strauss et al. 2002). These are, of course, the objects most likely to be of interest in a mergers study though many might be projections, so one cannot assume they are part of a perturbed system.

We argue now that our estimate for the fraction of ‘strongly-perturbed’ volume-limited MGS objects, f_{mgs} , is a good approximation to the ‘real’ fraction of volume-limited galaxies. For simplicity, let us begin with a sky as depicted in Figure A1 involving only galaxies which are bright enough to be spectral targets and where some of these might be in the process of a binary merger such that they are within $55''$ of another spectral target. We assume that mergers are randomly distributed with respect to tile-overlap regions. Let the number of single (i.e. non-perturbed) galaxies be N_s and the number of binary-merger *pairs* be N_m . The merger fraction that we calculated, f_{mgs} would therefore be

$$f_{mgs} = \frac{2k_{sky}N_m + (1 - k_{sky})N_m}{2k_{sky}N_m + (1 - k_{sky})N_m + N_s} \quad (A1)$$

$$= \frac{N_m(1 + k_{sky})}{N_m(1 + k_{sky}) + N_s}. \quad (A2)$$

The real merger fraction should take account of everything regardless of overlap regions so that the fraction of strongly perturbed spectral targets is

$$f_{real} = \frac{2N_m}{2N_m + N_s}. \quad (A3)$$

Now we let the ratio of binary-merger pairs N_m to single galaxies in the local universe equal p . Taking the ratio of (A2) and (A3) and substituting $N_m = pN_s$ will give the corrective factor, C , relating our fraction to the real fraction:

$$C(k_{sky}, p) = \frac{f_{real}}{f_{mgs}} = \frac{2(1 + pk_{sky} + p)}{(2p + 1)(1 + k_{sky})}. \quad (A4)$$

When $k_{sky} = 1$ (i.e. when the whole sky is an overlap region) we get $f_{real} = f_{mgs}$. For realistic values like $k_{sky} \sim 30\%$, $p \sim 5\%$ we get a ratio $C(k_{sky} = 0.3, p = 0.05) \sim 1.5$ and we find that (A4) is not very sensitive to changes in p . Multi-mergers have the affect of increasing C but are rare enough to be ignored and so we can take our corrective factor to be $C = 1.5$.

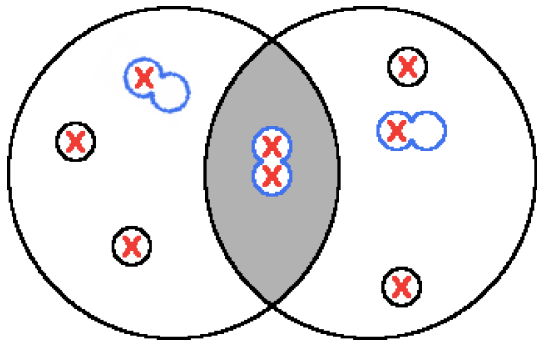


Figure A1. An illustration of the SDSS spectroscopic tiling scheme. The overlap region shaded grey covers a fraction k_{sky} of the area. Strongly-perturbed systems are coloured with blue outlines and single galaxies black. Those targets which receive spectra are marked with a red cross. Here we only consider systems where some strongly-perturbed spectral objects are merging with spectral targets.

are able to filter out more actual ‘strongly-perturbed’ systems. However, we again needed to decide a cutoff for the vote fraction, f'_m . We examined twenty sets of ten images across the entire f'_m range and estimated how many of these were genuine ‘strongly-perturbed’ systems. We found that $\gtrsim 80\%$ of images were actual ‘strongly-perturbed’ systems for $f'_m > 0.6$ and, following Lintott et al. (2008), made this number the cut off. The fraction of objects with $f'_m > 0.6$ is $\sim 53\%$ which is in good agreement with our estimate that 50 – 59% of objects in this range are ‘strongly perturbed.’

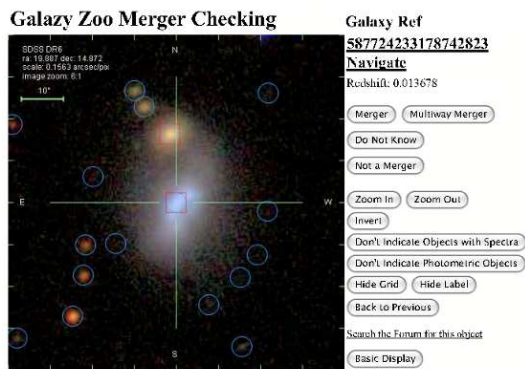


Figure B1. A Galaxy Zoo Mergers interface was established with the specific goal to assess GZ images that had been classified as belonging to the $0.2 < f_m < 0.4$ bin.

APPENDIX B: EXAMINATION OF THE $0.2 < F_M < 0.4$ MERGER FRACTION

In estimating the merger fraction of the local universe, we needed to estimate the percentage of ‘strongly-perturbed’ galaxies in the range $0.0 < f_m < 0.4$ which we handled by selecting bins of 100 images and visually inspecting them. Given the enthusiasm of public users, we also decided to make available those images already classified as $0.2 < f_m < 0.4$ with extended advice on spotting mergers in order that they might assist in this specific task. This led to the establishment of a sister-site dedicated to the assessment of candidate merger images that offered users more information in order to make an informed decision. This removes the ambiguity of whether or not to classify an image according to its morphology or whether it is merging or not - a dichotomy arising from the simplicity of the GZ interface. The mergers-interface is shown in Figure B1.

After a few months, enough users had re-classified these images of interest in order that a new-weighted-merger-vote fraction, f'_m , could be calculated for each image based upon clicks of the ‘merger,’ ‘not-merger’ and ‘don’t know’ buttons. By then volume-limiting all spectral objects from this sample as before with $0.005 < z < 0.1$ and $M_r < -20.55$ we